

Computing Surface Hyperbolic Structure and Real Projective Structure

Miao Jin^{*}
Stony Brook University

Feng-Luo[†]
Rutgers University

Xianfeng Gu[‡]
Stony Brook University

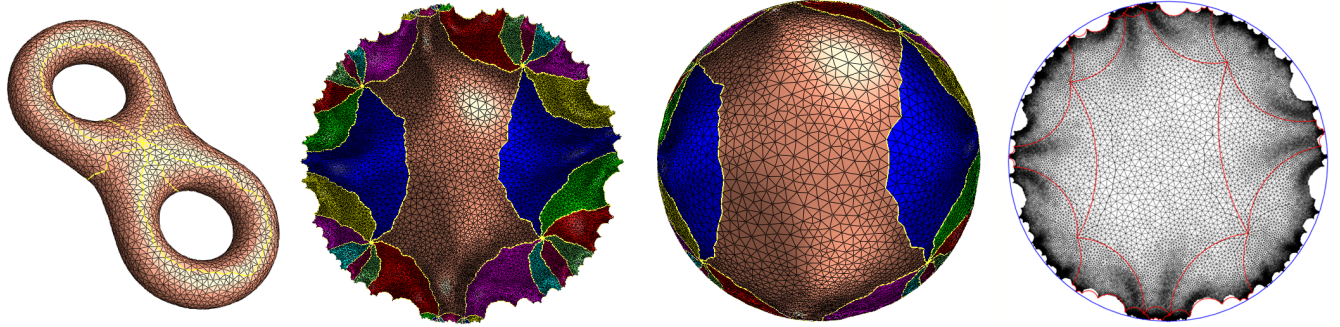


Figure 1: The hyperbolic structure and real projective structure of a genus two closed surface. From left to right, the original surface with a set of canonical fundamental group basis; the isometric embedding of its universal covering space in the Poincaré disk with the hyperbolic uniformization metric; the isometric embedding in the Klein disk which induces the real projective structure; the isometric embedding in the Poincaré disk, where the boundaries of fundamental domains are straightened to hyperbolic lines.

Abstract

Geometric structures are natural structures of surfaces, which enable different geometries to be defined on the surfaces. Algorithms designed for planar domains based on a specific geometry can be systematically generalized to surface domains via the corresponding geometric structure. For example, polar form splines with planar domains are based on affine invariants. Polar form splines can be generalized to manifold splines on the surfaces which admit affine structures and are equipped with affine geometries.

Surfaces with negative Euler characteristic numbers admit hyperbolic structures and allow hyperbolic geometry. All surfaces admit real projective structures and are equipped with real projective geometry. Because of their general existence, both hyperbolic structures and real projective structures have the potential to replace the role of affine structures in defining manifold splines.

This paper introduces theoretically rigorous and practically simple algorithms to compute hyperbolic structures and real projective structures for general surfaces. The method is based on a novel geometric tool - *discrete variational Ricci flow*. Any metric surface admits a special uniformization metric, which is conformal to its original metric and induces constant curvature. Ricci flow is an efficient method to calculate the uniformization metric, which determines the hyperbolic structure and real projective structure.

The algorithms have been verified on real surfaces scanned from sculptures. The method is efficient and robust in practice. To the best of our knowledge, this is the first work of introducing algorithms based on Ricci flow to compute hyperbolic structure and real projective structure.

More importantly, this work introduces the framework of general geometric structures, which enable different geometries to be defined on manifolds and lay down the theoretical foundation for many important applications in geometric modeling.

CR Categories: I.3.5 [Computer Graphics]: Computational Geometry and Object Modeling—Geometric algorithms;

Keywords: Geometric Structures, Hyperbolic Structure, Real Projective Structure, Hyperbolic geometry, Real Projective Geometry, Affine Geometry, Ricci Flow, Riemann Uniformization

1 Introduction

According to Felix Klein's Erlanger program, a geometry is the study of properties of a space X invariant under a group G of transformations of X . For example, planar Euclidean geometry is the geometry of 2-dimensional Euclidean space \mathbb{R}^2 invariant under rigid motions (translations, rotations). The central invariant is the distance between any two points. Planar affine geometry studies the invariants of the plane under affine transformations (non singular linear maps), where the invariants are parallelism, barycentric coordinates. Real projective geometry on real projective space \mathbb{RP}^2 studies the invariants under projective transformation (linear rational maps), where the cross ratio is the central invariant.

^{*}e-mail: mjin@cs.sunysb.edu

[†]e-mail: fluo@math.rutgers.edu

[‡]e-mail: gu@cs.sunysb.edu

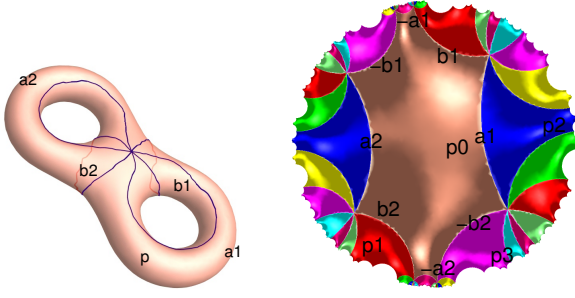


Figure 2: A genus two surface with a set of canonical fundamental group generators $\{a_1, b_1, a_2, b_2\}$ is on the left. A finite portion of its universal covering space is shown on the right. Different fundamental domains are colored differently. The boundary of each fundamental domain is the preimage of $a_1b_1a_1^{-1}b_1^{-1}a_2b_2a_2^{-1}b_2^{-1}$. $\{p_0, p_1, p_2\}$ are preimages of p .

Most algorithms in geometric modeling, computational geometry and computer graphics are constructed on planar spaces, in which different algorithms are based on different geometries. For example, planar Delaunay triangulation uses Euclidean geometry, and the distances among points play the central role; Splines with planar domains based on polar forms use affine geometry, and barycentric coordinates play central roles. The fundamental task of geometric modeling is to study shapes, therefore it is highly desirable to find a systematic way to generalize the conventional mature planar constructions onto the surfaces. Hence, we need a solid theoretical tool to define different geometries on surfaces.

Geometric structures are natural surface structures, which enable different geometries to be defined on surfaces coherently and allow general planar algorithmic constructions to be generalized onto surfaces directly.

1.1 Geometric Structures

Surfaces are *manifolds*, where no global coordinates exist in general. Instead, a manifold M is covered by a set of open sets $\{U_\alpha\}$. Each U_α can be parameterized by a local coordinate system and a map $\phi_\alpha : U_\alpha \rightarrow \mathbb{R}^2$ maps U_α to its parameter domain. (U_α, ϕ_α) is a local chart for the manifold M . A particular point p may be covered by two local coordinate systems (U_α, ϕ_α) and (U_β, ϕ_β) . The transformation of the local coordinates of p in (U_α, ϕ_α) to those in (U_β, ϕ_β) is formulated as the chart transition map $\phi_{\alpha\beta} = \phi_\beta \circ \phi_\alpha^{-1}$. All the charts form an *atlas* $\{(U_\alpha, \phi_\alpha)\}$.

If all chart transition maps are rigid motions on \mathbb{R}^2 , then we can discuss the concepts of angle, distance, and parallelism on the surface locally. These geometric measurements can be calculated on one chart, but the results are independent of the choice of the chart. Namely, we can define Euclidean geometry on the surface. Similarly, if all transition maps are affine, then we can define parallelism and midpoint of a line segment on the surface. If all transition maps belong to a particular transformation group of \mathbb{R}^2 , we can define the corresponding geometry on the surface. We say a surface M has a (X, G) structure, where X is a topological space, G is a subgroup of the transformation group of X , if M has an atlas $\{(U_\alpha, \phi_\alpha)\}$,

such that the parameter domain $\phi_\alpha(U_\alpha) \subset X$ is in space X , and the transition maps $\phi_{\alpha\beta} \in G$ are in G .

Surfaces have rich (X, G) geometric structures. A genus zero surface has a spherical structure, where X is the unit sphere \mathbb{S}^2 and G is the rotation group. A genus one surface has an affine structure, which plays vital roles in manifold splines. For an affine structure, X is the plane \mathbb{R} and G is the general linear maps $GL(\mathbb{R}, 2)$.

Besides (X, G) structures, surfaces have more geometric structures, such as *topological structures*, *differential structures*, and *conformal structures*.

1.2 Hyperbolic Structure and Real Projective Structure

This paper focuses on hyperbolic structures and real projective structures. For hyperbolic structure, X is the hyperbolic space \mathbb{H}^2 and G is the group of rigid motions on \mathbb{H}^2 . If we use Poincaré model for \mathbb{H}^2 , then G is the Möbius transformation group, (complex linear rational maps). For real projective structure, X is \mathbb{RP}^2 and G is the real projective maps $PGL(\mathbb{R}, 3)$, (real linear rational maps). Compared with the affine structure, whose transition maps are linear, hyperbolic and real projective structures have more complicate transition maps. But compared with other structures, such as differential and conformal structures, they have much simpler transition maps.

The existence of different (X, G) structures are determined by the topology of the surface. For example, a surface has an affine structure if and only if its Euler characteristic number is zero [Benzécri 1959; J.W.Milnor 1958]. Conventional polar form splines are based on affine geometry, therefore, it is impossible to generalize conventional splines on the surface without extraordinary points. Fortunately, all surfaces have real projective structures, and if a spline scheme is based on cross ratio, it can be generalized on surfaces directly.

Real projective structures are closely related to hyperbolic structures. Hyperbolic structures induce real projective structures in a natural way.

1.3 Previous Works

Geometric structures have been implicitly and explicitly applied in geometric modeling, computer graphics and medical imaging. For the genus zero case, the spherical structure was studied for texture mapping in [Gotsman et al. 2003; Praun and Hoppe 2003] and for conformal brain mappings in [Gu et al. 2004; Haker et al. 2000]. Algorithms for computing conformal structures were introduced in [Gu and Yau 2003; Jin et al. 2004], and the method is based on computing holomorphic differentials on surfaces.

Hyperbolic structure was applied in [Ferguson et al. 1992] for topological design of surfaces, where the high genus surfaces were represented as quotient spaces of the Poincaré disk over Fuchsian group actions. In [Grimm and Hughes 2003], Grimm and Hughes defined parameterizations for high genus surfaces and constructed functions on them. Wallner and Pottmann introduced the concept of spline orbifold in [Wallner and Pottmann 1997], which defined splines on three canonical parameter domains, the sphere, the plane and the Poincaré. The key difference between these works and our current one is

that our method computes the hyperbolic metric which is conformal to the original metric on the surface, but their works only consider the topology and ignore the geometry of the surface. For many real applications, such as texture mapping, shape analysis and spline constructions, conformality between the original and the final metrics is highly desirable.

Manifold splines based on polar forms are introduced in [Gu et al. 2005]. They demonstrated the equivalence between manifold splines and the affine structure and gave a systematic way to generalize splines defined on planar domains to manifold domains. They also constructed affine structures using conformal structures for surfaces with arbitrary topologies.

Recently, [Goldman 2003] examines some possible alternative mathematical foundations for Computer Graphics, such as Grassmann spaces and tensors. General geometric structures on manifolds contribute to the theoretical foundations for graphics and geometric modeling.

Ricci flow on surfaces was first introduced by Hamilton [Hamilton 1988]. Theoretical results of combinatorial Ricci flow have been summarized in [Chow and Luo 2003]. Conventional Ricci flow can be formulated as the gradient descent method for optimizing a special energy form, and the deficiency of its speed makes Ricci flow impractical. In our current work, we improved the theoretical results in [Chow and Luo 2003] by considering surface Riemannian metric induced from \mathbb{R}^3 instead of from the combinatorial structure. We replaced the gradient descent method with Newton's method to speedup Ricci flow completion by tens of times. We named this novel algorithm the *discrete variational Ricci flow*. A practical system for computing hyperbolic and real projective structures for real surfaces has been developed based on discrete variational Ricci flow.

Circle packing was first introduced by Thurston in the seventies in [Thurston 1976], with an algorithm. A practical software system for circle packing can be found in [Stephenson 2005]. The hyperbolic metrics computed in their system are not conformal to the original metrics. Recently, circle packing has been generalized to circle patterns [Bobenko and Schröder 2005] [Bobenko and Springborn 2004] and used for surface parameterization in [Kharevych et al. 2005], which focuses on Euclidean geometry. Circle packing, circle pattern and discrete Ricci flow can be unified using the derivative cosine law [Luo and Gu 2006].

Our current work is based on a novel theoretical tool - discrete variational Ricci flow and focuses on hyperbolic structure and real projective structure instead of Euclidean structure. Furthermore the hyperbolic metrics computed using our method are conformal to the original metrics. The conformal hyperbolic metrics convey much geometric information of the surfaces, which are valuable for the purposes of shape analysis.

1.4 Contribution

This paper introduces general geometric structures, such as the affine structure, the hyperbolic structure, and the real projective structure. Geometric structures allow different geometries to be defined on manifolds directly and lay down the theoretical foundations for graphics and geometric modeling.

Compared to other structures, the hyperbolic structure and real projective structure have not been fully studied. This paper

aims to introduce a novel practical algorithm to compute hyperbolic structure and real projective structure. The algorithm is based on a recently developed theoretical tool in differential geometry field- Ricci flow. To the best of our knowledge, this paper is the first to numerically compute hyperbolic structure using Ricci flow, and also the first one to introduce a practical method to compute real projective structures for arbitrary closed surfaces. Therefore, the major contributions of this paper are:

- Introduce a novel theoretical framework : Geometric Structures, which enable algorithms defined on Euclidean domains to be systematically generalized to manifold domains.
- Introduce a novel geometric tool : discrete Variational Ricci flow.
- Practical, efficient algorithm for computing hyperbolic structures for surfaces of genus at least two. The hyperbolic metric is conformal to the original metric on the surface.
- Practical and efficient algorithm to compute Real projective structures for arbitrary surfaces.

2 Theoretical Background

The algorithms require some basic concepts from algebraic topology, differential geometry and Riemann surface. We assume the readers are familiar with these subjects. In this section, we briefly review the basic concepts necessary for our discussion. For detailed explanation, we refer readers to [Thurston 1997].

2.1 (X, G) structure for Manifolds

Given a manifold S , suppose (U_α, ϕ_α) and (U_β, ϕ_β) are two charts, $U_\alpha \cap U_\beta \neq \emptyset$, then the chart transition is defined as

$$\phi_{\alpha\beta} : \phi_\alpha(U_\alpha \cap U_\beta) \rightarrow \phi_\beta(U_\alpha \cap U_\beta).$$

In what follows X will be a space with a geometry on it and G is the group of transformations of X which preserves this geometry. An atlas $\{U_\alpha, \phi_\alpha\}$ on a manifold is called (X, G) atlas if all chart transitions are in group G and the parameter domains $\phi_\alpha(U_\alpha)$ are in X , $\phi_\alpha(U_\alpha) \subset X$.

Two (X, G) atlases are *compatible*, if their union is still an (X, G) atlas. Compatible relation is an equivalent relation of atlases, and each equivalent class is called an (X, G) structure.

Any surface with negative Euler number has a hyperbolic structure $(\mathbb{H}^2, PGL(2, \mathbb{C}))$. Suppose $\{(U_\alpha, \phi_\alpha)\}$ is a hyperbolic atlas, then $\phi_\alpha(U_\alpha)$ is in the hyperbolic space and the transition maps are hyperbolic rigid motions. If we use Poincaré model, $\phi_{\alpha\beta}$ is a Möbius transformation.

Similarly, for a real projective atlas, the parameter domains are subsets of real projective space \mathbb{RP}^2 , and the transition maps are real projective transformations $PGL(3, \mathbb{R})$ (linear rational functions).

2.2 Riemann Surface Uniformization

Any orientated metric surface M has a special (\mathbb{C}, Ω) structure, where Ω represents the holomorphic functions on the complex plane. Namely, the chart transition maps are conformal maps. This structure is called the *conformal structure*. A surface with a conformal structure is called a *Riemann surface*.

Suppose a surface M is embedded in the Euclidean space \mathbb{R}^3 , then it has the Riemannian metric induced by the Euclidean metric, denoted as g_0 . A *conformal class of metrics* on M refers to a family of Riemannian metrics $\{e^{2\phi} g_0\}$ and the so called *conformal factor* $e^{2\phi}$ represents the area stretching under the metric $e^{2\phi} g_0$.

The Riemann Uniformization theorem claims that any Riemann surface M with metric g_0 admits a uniformization metric g , such that g and g_0 are conformal to each other $g = e^{2\phi} g_0$ and (M, g) has constant Gaussian curvature on the interior points and zero geodesic curvature on the boundary points. The constant Gaussian curvature is one of the three $\{-1, 0, 1\}$. Surfaces with positive Euler numbers have spherical uniformization metrics with $+1$ curvature; surfaces with zero Euler number have flat uniformization metrics with 0 curvature; surfaces with negative Euler numbers have hyperbolic uniformization metrics with -1 curvature. The uniformization metrics induce the spherical, Euclidean and hyperbolic structures on surfaces respectively.

2.3 Ricci flow

Surface Ricci flow is first introduced by Hamilton in [Hamilton 1988]. The main idea is to conformally deform the Riemannian metric of the surface driven by its curvature, then the metric will flow to the uniformization metric eventually.

Suppose M is a surface with the metric tensor $g = (g_{ij})$, and K is the current Gaussian curvature, then Ricci flow is defined as

$$\frac{\partial g_{ij}}{\partial t} = -2Kg_{ij}.$$

It is proven that the Ricci flow with normalized total surface area will flow the metric such that the Gaussian curvature on the surface is constant, namely the Gaussian curvature function $\lim_{t \rightarrow \infty} K(t, p)$ converges to a constant function. It is also proven that the convergence rate of Ricci flow is exponential, namely, for any point p on the surface,

$$|K(t, p) - K(\infty, p)| < c_1 e^{-c_2 t},$$

where c_1, c_2 are two constants determined by the surface itself.

2.4 Fundamental Group and Universal Covering Space

If two closed curves on surface M can deform to each other without leaving the surface, they are homotopic to each other. The closed loops on the surface can be classified by homotopic classes. Two closed curves sharing common points can be concatenated to form another loop. This operation defines the multiplication of homotopic classes naturally. Therefore, all the base pointed homotopy classes form the so called *the first fundamental group* of M , and is denoted as $\pi_1(M)$. For genus g closed surface, the fundamental group has $2g$ generators. A set of fundamental group basis $\{a_1, b_1, a_2, b_2, \dots, a_g, b_g\}$ is

canonical, if a_i, b_i have one geometric intersection, but a_i, a_j have zero geometric intersection, and a_i, b_j have zero geometric intersection. (The definition of geometric intersection number between two simple curves a, b is the $\min\{|x \cap y| : x \text{ homotopic to } a, y \text{ homotopic to } b\}$.)

Suppose that \bar{M} and M are surfaces. Then (\bar{M}, π) is said to be a covering space of M if π is a surjective continuous map with every $p \in M$ having an open neighborhood U such that every connected component of $\pi^{-1}(U)$ is mapped homeomorphically onto U by π . Furthermore, if \bar{M} is simply connected, (\bar{M}, π) is the universal covering space of M .

A transformation of the universal covering space $\phi : \bar{M} \rightarrow \bar{M}$ is a *deck transformation*, if $\pi = \pi \circ \phi$. All deck transformations form a group G , the so called *Fuchsian group* of M , which is isomorphic to the fundamental group of M in the following way. Suppose $p \in M$ is an arbitrary point on M , its preimages are $\pi^{-1}(p) = \{p_0, p_1, p_2, \dots, p_n, \dots\}$ on \bar{M} . Suppose a deck transformation $\phi \in G$ maps p_0 to p_k . Then we can draw a curve segment on the universal covering space $\gamma : [0, 1] \rightarrow \bar{M}$ connecting p_0, p_k and its projection $\pi(\gamma)$ is a loop on M , the homotopy class of γ is determined by p_0, p_k only and independent of the choice of γ . Then we get a bijective map from deck transformations to the first fundamental group of M .

A *fundamental domain* F is a subset of \bar{M} , such that the universal covering space is the union of conjugates of F , $S = \bigcup_{g \in G} gF$, and any two conjugates have no interior point in common. Given a canonical fundamental group generators $\{a_i, b_i\}$, where $i = 1, 2, \dots, g$, we can slice M along the curves and get a fundamental domain with boundary

$$\{a_1 b_1 a_1^{-1} b_1^{-1} a_2 b_2 a_2^{-1} b_2^{-1} \cdots a_g b_g a_g^{-1} b_g^{-1}\}.$$

Suppose a surface M has genus at least two with a hyperbolic metric, its universal covering space \bar{M} can be isometrically embedded in the hyperbolic space. The embedding produces a tessellation of the hyperbolic space, and each tile is a fundamental domain. The deck translations which map fundamental domains to fundamental domains are rigid motions in the hyperbolic space. Figure 2 illustrates the fundamental group generators of a genus two surface and its universal covering space.

2.5 Hyperbolic Space Models

There are two common models for hyperbolic geometry.

2.5.1 Poincaré Model

The Poincaré model is a unit disk \mathbb{D}^2 in the complex plane with the Riemannian metric $ds^2 = \frac{4dzd\bar{z}}{(1-z\bar{z})^2}$.

The geodesics are circular arcs perpendicular to the boundary of the unit disk $\partial\mathbb{D}^2$. The isometric transformations in this model is the so called Möbius transformation with the form

$$\phi(z) = e^{i\theta} \frac{z - z_0}{1 - \bar{z}_0 z}, z, z_0 \in \mathbb{C}, \theta \in [0, 2\pi).$$

The above Möbius transformation maps z_0 to the center of the disk, and rotate the whole disk by angle θ . Hyperbolic circles are also Euclidean circles.

Suppose M is a closed surface with genus $g > 1$, then M has a hyperbolic uniformization metric. The universal covering space \tilde{M} with this metric is isometric to \mathbb{H}^2 . Each fundamental domain is a polygon with $4g$ sides and each side is a hyperbolic geodesic. This forms a tessellation of \mathbb{H}^2 . The deck transformations of \tilde{M} are Möbius transformation on \mathbb{H}^2 .

The Poincaré model is a conformal model, whereas the Klein model is a real projective model.

2.5.2 Klein Model

The Klein model is another model of hyperbolic space defined also on the unit disk \mathbb{D}^2 . Any geodesic in the Klein model is a chord of the unit circle of the boundary of \mathbb{D}^2 . The map from the Poincaré model to the Klein model is $\beta : \mathbb{H}^2 \rightarrow \mathbb{D}^2$,

$$\beta(z) = \frac{2z}{1 + \bar{z}z}, \beta^{-1}(z) = \frac{1 - \sqrt{1 - \bar{z}z}}{\bar{z}z} z. \quad (1)$$

Any Möbius transformation in the Poincaré model ϕ becomes a real projective transformation in the Klein model $\beta \circ \phi \circ \beta^{-1}$.

3 Hyperbolic Discrete Variational Ricci flow

This section explains the algorithms to compute the hyperbolic uniformization metric of a surface with negative Euler number. In practice, all surfaces are represented as triangular meshes.

A triangular mesh is a two dimensional simplicial complex, denoted by $M = (V, E, F)$, where V is the set of all vertices, E is the set of all non-oriented edges and F is the set of all faces. We use $v_i, i = 1, \dots, n$ to denote its vertices, e_{ij} to denote an oriented edge from v_i to v_j , and f_{ijk} to denote an oriented face with vertices v_i, v_j, v_k which are ordered counter-clockwisely such that the face normals toward outside.

In reality, surfaces are approximated by meshes. The concepts of conformal maps, hyperbolic metrics and Ricci flow are also translated from the smooth surface category to the discrete mesh category. We show the Riemannian metrics of meshes induced by Delaunay triangulations converge to the metric on the smooth surface in [Dai et al. 2006]. The convergence of conformal structures is proved in [Luo 2006]. The convergence of hyperbolic structure remains open.

3.1 Circle Packing Metric

The following key observation plays vital role for systematically translating smooth Ricci flow to discrete Ricci flow. A conformal mapping between two smooth surfaces maps infinitesimal circles to other infinitesimal circles, changing the radii of the infinitesimal circles, but preserving the intersection angles among them.

In order to translate conformal mappings from the smooth surface category to the discrete mesh category, Thurston defined *circle packing* as the following,

1. Change infinitesimal circles to circles with finite radii.
2. Each circle is centered at a vertex like a cone, and the radius is denoted as γ_i for vertex v_i .

3. An edge has two vertices. The two circles intersect each other with an intersection angle, and the angle is denoted as Φ_{ij} for edge e_{ij} , called the *weight*.

Therefore a mesh with circle packing (M, Γ, Φ) , where M represents the triangulation (connectivity), $\Gamma = \{\gamma_i, v_i \in V\}$ are the vertex radii and $\Phi = \{\Phi_{ij}, e_{ij} \in E\}$ are the angles associated with each edge. A *discrete conformal mapping* $\tau : (M, \Gamma, \Phi) \rightarrow (M, \tilde{\Gamma}, \tilde{\Phi})$ solely changes the vertex radii Γ , but preserves the intersection angles Φ .

In reality, a discrete conformal mapping can approximate a smooth conformal mapping with arbitrary accuracy. If we keep subdividing the mesh and construct refiner and refiner circle packing, the discrete conformal mappings will converge to the smooth conformal mapping. For a rigorous proof, we refer the readers to [Rodin and Sullivan 1987].

A circle packing (M, Φ, Γ) uniquely determines a so called *circle packing metric*. The length l_{ij} associated with the edge e_{ij} is computed using the cosine law,

$$l_{ij} = \sqrt{\gamma_i^2 + \gamma_j^2 + 2\gamma_i\gamma_j \cos \Phi_{ij}}. \quad (2)$$

In practice, the mesh is embedded in \mathbb{R}^3 , the mesh has an induced Euclidean metric, the Euclidean length of edge e_{ij} is denoted as \bar{l}_{ij} . We select an appropriate circle packing metric (Γ, Φ) , such that it approximates the Euclidean metric as close as possible,

$$\min_{\Gamma, \Phi} \sum_{e_{ij} \in M} |l_{ij} - \bar{l}_{ij}|^2.$$

Given a circle packing metric on a mesh, such that the edge lengths for each face f_{ijk} satisfy the triangle inequality $l_{ij} + l_{jk} > l_{ki}$, then the face can be realized in the hyperbolic space. We denote the angle at vertex v_i as θ_i^{jk} and compute it by the hyperbolic cosine law:

$$\cos \theta_i^{jk} = \frac{\cosh l_{ij} \cosh l_{ik} - \cosh l_{jk}}{\sinh l_{ij} \sinh l_{ik}}.$$

The discrete Gaussian curvature K_i at an interior vertex v_i is defined as

$$K_i = 2\pi - \sum_{f_{ijk} \in F} \theta_i^{jk}, \quad v_i \notin \partial M, \quad (3)$$

while the discrete Gaussian curvature for a boundary vertex v_i is defined as

$$K_i = \pi - \sum_{f_{ijk} \in F} \theta_i^{jk}, \quad v_i \in \partial M. \quad (4)$$

3.2 Hyperbolic Ricci Flow

Given a mesh with circle packing metric (M, Γ, Φ) , the discrete hyperbolic Ricci flow is defined as

$$\frac{\partial \gamma_i}{\partial t} = -\sinh \gamma_i K_i \quad (5)$$

A solution to equation 5 exists and is *convergent*

$$\lim_{t \rightarrow \infty} K_i(t) = 0.$$

A convergent solution *converges exponentially* if there are positive constants c_1, c_2 , so that for all time $t \geq 0$

$$|K_i(t) - K_i(\infty)| \leq c_1 e^{-c_2 t}, |\gamma_i(t) - \gamma_i(\infty)| \leq c_1 e^{-c_2 t}.$$

In theory, the discrete Ricci Flow is guaranteed to be exponentially convergent [Chow and Luo 2003].

3.3 Hyperbolic Discrete Variational Ricci flow Using Newton's Method

Discrete hyperbolic Ricci Flow is the solution to an energy optimization problem, namely, it is the negative gradient flow of some convex energy, which was first introduced by [de Verdière 1991] for tangential circle packing, and [Chow and Luo 2003] generalizes it to all intersection cases. Therefore we can use Newton's method to further improve the convergence speed.

Let $u_i = \ln \tanh \frac{\gamma}{2}$, under this change of variable, the Ricci Flow in Equation 5 takes the following form: $\frac{du_i}{dt} = -K_i$,

We can define an energy form

$$f(\mathbf{u}) = \int_{\mathbf{u}_0}^{\mathbf{u}} \sum_{i=1}^n K_i du_i,$$

where $\mathbf{u} = (u_1, u_2, \dots, u_n)$, \mathbf{u}_0 is $(0, 0, \dots, 0)$. Thus $\frac{\partial f}{\partial u_i} = K_i$, that is, the Ricci Flow 5 is the negative gradient flow of the energy $f(\mathbf{u})$.

The Hessian matrix of the energy f is

$$\frac{\partial^2 f}{\partial u_i \partial u_j} = \frac{\partial K_i}{\partial u_j} = \frac{\partial K_i}{\partial r_j} \sinh r_j,$$

From the definition of curvature K_i , hyperbolic cosine law and the definition of circle packing metric, the above formulae has a closed form. The Hessian matrix can be easily verified to be positive definite. As f is strictly convex, it therefore has a unique global minimum, so Newton's method can be used to stably locate this minimum.

4 Computing Hyperbolic Structures

After computing the hyperbolic uniformization metrics described in the last section 3, we focus on computing hyperbolic structures of general surfaces in the current section.

For any surface with boundaries, we can convert it to a closed symmetric surface using the double covering method [Gu and Yau 2003]. First we make two copies of the surface, then we reverse the orientation of one of them and glue the two copies along their corresponding boundaries. The double covered surface admits a uniformization metric conformal to its original metric and the original boundary curves become geodesics under this metric. The real projective structures of the original surface and its double covering can be induced by this uniformization metric. Therefore, in the following discussion, we always assume the surfaces are closed unless otherwise noted.

4.1 Algorithm Pipeline

In order to compute the hyperbolic structure, we develop the following algorithms. Suppose M is a surface with genus g greater than one with hyperbolic uniformization metric, which is computed in the previous section, the major steps for computing a hyperbolic atlas of M are

1. Compute the fundamental domain of the surface M ; construct a finite portion of its universal covering space (\bar{M}, π) , π is the projection map; construct a canonical fundamental group generators $\Gamma = \{a_1, b_1, \dots, a_g, b_g\}$.
2. Isometrically embed the universal covering space (or a fundamental domain) onto the Poincaré disk.
3. Compute the Fuchsian group generators (deck transformation group of \bar{M}) corresponding to a_i, b_i , denoted them as $\{\phi_1, \phi_2, \dots, \phi_{2g}\}$, where ϕ_i 's are Möbius transformation on the Poincaré disk.
4. Construct a hyperbolic atlas

The algorithms in the first step, such as computing the fundamental domain, universal covering space and canonical homology basis, have been studied in computational topology and computer graphics literature [Colin de Verdière and Lazarus 2002] [Erickson and Whittlesey 2005]. We adopted the methods introduced in [Carner et al. 2005]. The following discussion will explain the other steps in detail.

4.2 Hyperbolic Embedding

In the second step, we need to isometrically embed the universal covering space \bar{M} in the Poincaré disk. Let the isometric embedding be

$$\phi : \bar{M} \rightarrow \mathbb{H}^2. \quad (6)$$

First, we select a face f_{012} from \bar{M} arbitrarily. Suppose three edge lengths are $\{l_{01}, l_{12}, l_{20}\}$, the corner angles are $\{\theta_0^{12}, \theta_1^{20}, \theta_2^{01}\}$ under the hyperbolic uniformization metric. We can simply embed the triangle as

$$\phi(v_0) = 0, \phi(v_1) = \frac{e^{l_{01}} - 1}{e^{l_{01}} + 1}, \phi(v_2) = \frac{e^{l_{02}} - 1}{e^{l_{02}} + 1} e^{j\theta_0^{12}}.$$

Second, we can embed all the faces which share an edge with the first embedded face. Suppose a face f_{ijk} is adjacent to the first face, vertices v_i, v_j have been embedded. A hyperbolic circle is denoted as (\mathbf{c}, r) , where \mathbf{c} is the center, r is the radius. Then $\phi(v_k)$ should be one of the two intersection points of $(\phi(v_i), l_{ik})$ and $(\phi(v_j), l_{jk})$. Also, the orientation of $\phi(v_i), \phi(v_j), \phi(v_k)$ should be counter-clock-wise. In Poincaré model, a hyperbolic circle (\mathbf{c}, r) coincides with an Euclidean circle (\mathbf{C}, R) ,

$$\mathbf{C} = \frac{2 - 2\mu^2}{1 - \mu^2|\mathbf{c}|^2} \mathbf{c}, R^2 = |\mathbf{C}|^2 - \frac{|\mathbf{c}|^2 - \mu^2}{1 - \mu^2|\mathbf{c}|^2},$$

where $\mu = \frac{e^r - 1}{e^r + 1}$. The intersection points between two hyperbolic circles can be found by intersecting the corresponding Euclidean circles. The orientation of triangles can also be determined using Euclidean geometry on the Poincaré disk.

Then, we can repeatedly embed faces which share edges with embedded faces in the same manner, until we embed enough portions of the whole of \bar{M} to the Poincaré disk.

4.3 Fuchsian Group Generator

Let $\pi(M)$ be the fundamental group of M , with a set of canonical basis $\Gamma = \{a_1, b_1, \dots, a_g, b_g\}$, while all curves only share one base point as shown in the left frame of figure 2. For each closed curve $\gamma : [0, 1] \rightarrow M$ on M , $\gamma(0) = \gamma(1)$, we use $[\gamma]$ to denote its homotopy class.

Let (\bar{M}, π) be the universal covering space embedded in the Poincaré disk as shown in the right frame of figure 2. Let $\bar{p}, \bar{q} \in \bar{M}$ be two points, such that $\pi(\bar{p}) = \pi(\bar{q})$. Suppose $\bar{\gamma} : [0, 1] \rightarrow \bar{M}$ is a curve, such that $\bar{\gamma}(0) = \bar{p}, \bar{\gamma}(1) = \bar{q}$, then $\pi(\bar{\gamma})$ is a closed loop on M . Its homotopy class is $[\pi(\bar{\gamma})]$. It can be verified that $[\pi(\bar{\gamma})]$ is determined by \bar{p} and \bar{q} , independent of the choice of $\bar{\gamma}$, therefore, we use $[\bar{p}, \bar{q}]$ to denote the homotopy class of $[\pi(\bar{\gamma})]$.

Given a base point on the surface $p \in M$, its preimages are $\pi^{-1}(p) = \{\bar{p}_0, \bar{p}_1, \bar{p}_2, \dots\} \subset \bar{M}$. Then $[\bar{p}_0, \bar{p}_k], k = 0, 1, 2, \dots$ will traverse the whole fundamental group $\pi(M)$. For each k , there exists a unique deck transformation $\tau_k : \bar{M} \rightarrow \bar{M}$, such that $\tau_k(\bar{p}_0) = \tau_k(\bar{p}_k)$, furthermore, τ_k is a Möbius transformation. The group formed by $\{\tau_k\}$ is called the *Fuchsian group* of M , and denoted as $F(M)$. Then we construct a map η between the fundamental group $\pi(M)$ and the Fuchsian group $F(M)$,

$$\eta : \pi(M) \rightarrow F(M), [\bar{p}_0, \bar{p}_k] \rightarrow \tau_k.$$

It can be verified that the map is an isomorphism.

The goal of the algorithm in this subsection is to compute the isomorphism η . It is sufficient to find the Möbius transformations corresponding to the curves in Γ .

First we choose two distinct points p and q on the surface, $p, q \in M$, such that p, q are not on any curves in Γ , $p, q \notin \Gamma$. The preimages of Γ $\pi(\Gamma)$ partition the covering space \bar{M} to fundamental domains, $\{\Sigma_0, \Sigma_1, \Sigma_2, \dots\}$. The preimages of p and q are

$$\pi^{-1}(p) = \{\bar{p}_k\}, \pi^{-1}(q) = \{\bar{q}_k\}, k = 0, 1, 2, \dots,$$

both \bar{p}_k and \bar{q}_k are interior points of Σ_k .

Suppose Σ_0 and Σ_1 are two fundamental domains on \bar{M} adjacent to each other, $\pi(\Sigma_0 \cap \Sigma_1) = a_2$. There exists a unique Möbius transformation ψ_1 , such that $\psi_1(\bar{p}_0) = \bar{p}_1, \psi_1(\bar{q}_0) = \bar{q}_1$. In order to compute ψ_1 , we construct a Möbius transformation μ_0 to map \bar{p}_0 to the origin, \bar{q}_0 to a real positive number, and μ_1 to map \bar{p}_1 to the origin and \bar{q}_1 to the same positive number, then

$$\psi_1 = \mu_1 \circ \mu_0^{-1}.$$

Therefore the problem is deduced to find a Möbius transformation μ , such that for a given pair of complex numbers inside the Poincaré disk $z_0, z_1 \in \mathbb{H}^2$,

$$\mu(z_0) = 0, \arg(\mu(z_1)) = 0.$$

μ can be constructed straightforwardly,

$$\mu = e^{-i\theta_0} \frac{z - z_0}{1 - \bar{z}_0 z}, \theta_0 = \arg \frac{z_1 - z_0}{1 - \bar{z}_0 z_1}.$$

In this way, by choosing different Σ_k 's adjacent to Σ_0 , we can compute all the Möbius transformations ψ_k which are the

generators of the Fuchsian group of M . The isomorphism $\eta : \pi(M) \rightarrow F(M)$ can be constructed in the following way:

$$\eta(a_i) = \tau_k, if [\pi(\Sigma_0 \cap \Sigma_k)] = [b_i^{-1}],$$

and

$$\eta(b_i) = \tau_k, if [\pi(\Sigma_0 \cap \Sigma_k)] = [a_i].$$

4.4 Hyperbolic Atlas

First we construct a family of open sets $\{U_\alpha\}$, such that the union of the open sets covers the surface M , $M \subset \bigcup U_\alpha$. Then we locate one preimage of each U_α in the universal covering space $\bar{M}, \pi^{-1}(U_\alpha)$. The embedding of the preimage $\pi^{-1}(U_\alpha)$ in the Poincaré disk gives the local coordinates of U_α , namely

$$\phi_\alpha := \phi \circ \pi^{-1},$$

where ϕ is the embedding map defined in equation 6. If one point $p \in M$ on the surface M is covered by two charts (U_α, ϕ_α) and (U_β, ϕ_β) , suppose $\bar{p}_\alpha \in \pi^{-1}(U_\alpha)$ and $\bar{p}_\beta \in \pi^{-1}(U_\beta)$, and the homotopy class $[\bar{p}_\alpha, \bar{p}_\beta] = [\gamma_1 \gamma_2 \cdots \gamma_n]$, then the chart transition map $\phi_{\alpha\beta}$ has the form

$$\phi_{\alpha\beta} = \eta(\gamma_n) \circ \eta(\gamma_{n-1}) \cdots \eta(\gamma_1),$$

where $\gamma_k, k = 1, 2, \dots, n$ are fundamental group generators, $\gamma_k \in \Gamma$. $\phi_{\alpha\beta}$ is Möbius transformation on the Poincaré disk. Therefore $\{(U_\alpha, \phi_\alpha)\}$ is a hyperbolic atlas.

5 Computing Real Projective Structure

Any oriented metric surface has a real projective structure. Real projective structures are induced by spherical structures, Euclidean structures and hyperbolic structures. This section introduces the algorithms to compute real projective atlases for surfaces with different topologies.

5.1 Genus zero surfaces

Closed genus zero surfaces have spherical structures. The universal covering space of a closed genus zero surface is itself. Therefore, the surface can be conformally mapped to the unit sphere.

A method based on heat flow to construct conformal maps between a closed genus zero surface to the unit sphere S^2 is introduced in [Gu et al. 2004]. The spherical uniformization metrics are induced by these conformal maps.

We set six tangent planes at the intersection points between the unit sphere and the axes, then project the sphere onto these tangent planes using central projection. This procedure produces the real projective atlas for the surface.

Figure 10 demonstrates a real projective atlas for a closed genus zero surface, Michelangelo's David head model.

5.2 Genus one surfaces

Any genus one oriented surface admits a flat uniformization metric, such that the Gaussian curvature is zero everywhere. Its universal covering space can be embedded in the plane. Each fundamental domain is a parallelogram, and the deck transformations are translations on the plane.

The flat uniformization metric on a genus one closed surface can be induced by the holomorphic 1-forms on it. A holomorphic 1-form can be treated as a pair of vector fields with zero divergence and circulation, and are orthogonal to each other. The algorithms for computing holomorphic 1-forms are introduced in [Gu and Yau 2003; Gu et al. 2005]. By integrating a holomorphic 1-form, its universal covering space can be conformally mapped to the plane. This induces an affine atlas for the surface. This construction method is similar to the algorithms in section 4. Affine structure can be treated as a special case of real projective structure.

5.3 High genus surfaces

For a closed surface M with genus $g > 1$, from its hyperbolic structure we can deduce its real projective atlas. But the real projective structure can not deduce the hyperbolic structure. Suppose $\{(U_\alpha, \phi_\alpha)\}$ is a hyperbolic atlas of M , a real projective atlas $\{(U_\alpha, \tau_\alpha)\}$ can be straightforwardly constructed. Let

$$\tau_\alpha = \beta \circ \phi_\alpha,$$

and

$$\tau_{\alpha\beta} = \beta \circ \phi_{\alpha\beta} \circ \beta^{-1}.$$

where β is the map from the Poincaré model to the Klein model as defined in equation 1. Suppose $\phi_{\alpha\beta}$ has the form

$$\phi_\alpha = e^{i\theta} \frac{z - z_0}{1 - \bar{z}_0 z},$$

where $z_0 = x_0 + iy_0$. We use homogenous coordinates (xw, yw, w) to parameterize the points (x, y) on the Klein model, then the transition map $\tau_{\alpha\beta}$ has the following form $\tau_{\alpha\beta} = \frac{1}{\lambda} OT$, where $\lambda = x_0^2 + y_0^2 - 1$, O is the rotation matrix

$$O = \begin{pmatrix} \cos \theta & -\sin \theta & 0 \\ \sin \theta & \cos \theta & 0 \\ 0 & 0 & 1 \end{pmatrix}$$

and T is

$$T = \begin{pmatrix} 1 + x_0^2 - y_0^2 & 2x_0y_0 & -2x_0 \\ 2x_0y_0 & 1 - x_0^2 + y_0^2 & -2y_0 \\ 2x_0 & 2y_0 & -1 - x_0^2 - y_0^2 \end{pmatrix}.$$

6 Implementation

The algorithms are implemented using $c++$ on the windows platform. All the models are represented as triangular meshes and some of them are scanned from real sculptures. In order to manipulate the meshes efficiently, we use a common mesh library in our implementation: the OpenMesh [Sovakar and Kobbelt 2004] library, because it is flexible, efficient and versatile. In the following we demonstrate some of our experimental results.

Our experiments demonstrate that the hyperbolic discrete variational Ricci flow algorithms are efficient and Robust. Figure 9 shows the performance of Ricci flow on eight model. The upper blue curve is using hyperbolic Ricci flow with gradient descend method, compared to the lower red curve with Newton's method. It is obvious that Newton's method converges much faster.

Fuchsian group generators of eight model on Poincaré Model.

	$e^{i\theta}$	z_0
a_1	$-0.631374 + i0.775478$	$+0.730593 + i0.574094$
b_1	$+0.035487 - i0.999370$	$+0.185274 - i0.945890$
a_2	$-0.473156 + i0.880978$	$-0.798610 - i0.411091$
b_2	$-0.044416 - i0.999013$	$+0.035502 + i0.964858$

Fuchsian group generators of knotty model on Poincaré Model.

	$e^{i\theta}$	z_0
a_1	$-0.736009 + i0.676972$	$+0.844441 - i0.402575$
b_1	$+0.227801 - i0.973708$	$-0.851267 - i0.510906$
a_2	$-0.521197 + i0.853436$	$-0.528917 + i0.702150$
b_2	$-0.090798 - i0.995869$	$+0.973285 + i0.206533$

Figure 10 illustrates a genus zero closed surface case. First we conformally map the surface to a unit sphere, and induce the real projective atlas from its spherical image.

Figure 3 illustrates a genus one closed surface. We compute a holomorphic 1-form on the surface, which induces an affine structure. Figure (b) demonstrates one fundamental domain, (c) is a finite portion of its universal covering space with nine fundamental domains.

Figure 1 shows the process of computing hyperbolic atlas and real projective atlas for a genus two closed surface. Figure (a) is the original surface with 7000 faces, (b) is the isometric embedding of its universal covering space in the Poincaré disk with its hyperbolic uniformization metric, (c) shows the result after straightening the boundaries of fundamental domains to hyperbolic lines, (d) is the embedding in Klein model, which induces a real projective atlas. The most time consuming part is to compute its hyperbolic uniformization metric using discrete Ricci flow, which took 100 seconds on a 1.7G CPU plus 1M RAM laptop. So the total time for the whole process is no more than 2 minutes.

Figures 4,7,8 illustrate the same process for different genus two closed surfaces. Figure 5 demonstrates the isometric embedding of the universal covering space of a genus three surface, the scanned sculpture surface, on the Poincaré model and Klein model. Figure 6 is the same process for a genus four surface, a scanned Greek model. These results show our method is capable to handle surfaces with complicated geometries and topologies.

7 Conclusion

In this paper, we introduce a general framework to define different geometries on surfaces via geometric structures. Algorithms designed for Euclidean space can be systematically generalized to surface domains directly.

In order to compute hyperbolic structures and real projective structures on general surfaces, a theoretically rigorous and

Fuchsian group generators of eight model on Klein Model.

$$a_1 \begin{pmatrix} 10.3242 & 8.39204 & -13.2671 \\ -2.9578 & -1.08348 & 2.98706 \\ -10.6929 & -8.4024 & 13.6359 \end{pmatrix} \quad b_1 \begin{pmatrix} 4.86605 & -26.0235 & -26.4556 \\ 2.14144 & -5.86616 & -6.16422 \\ -5.22151 & 26.6577 & 27.1826 \end{pmatrix}$$

$$a_2 \begin{pmatrix} 6.59028 & 4.02982 & 7.65972 \\ -5.0888 & -1.69285 & -5.26893 \\ 8.26606 & 4.25502 & 9.35056 \end{pmatrix} \quad b_2 \begin{pmatrix} -0.963558 & -28.3933 & 28.392 \\ 1.08105 & 2.27398 & -2.31077 \\ -1.04743 & -28.4667 & 28.5035 \end{pmatrix}$$

Fuchsian group generators of Knotty model on Klein Model.

$$a_1 \begin{pmatrix} 5.45671 & -1.57356 & -5.59033 \\ -12.4179 & 6.33332 & 13.9038 \\ -13.527 & 6.4488 & 15.0189 \end{pmatrix} \quad b_1 \begin{pmatrix} -82.4315 & -50.31 & -96.5662 \\ 85.687 & 50.6147 & 99.5144 \\ 118.896 & 71.3578 & 138.669 \end{pmatrix}$$

$$a_2 \begin{pmatrix} -0.985119 & 2.85311 & -2.84793 \\ -4.65847 & 5.57247 & -7.19401 \\ 4.6553 & -6.18002 & 7.80157 \end{pmatrix} \quad b_2 \begin{pmatrix} -22.6068 & -5.81234 & 23.3206 \\ 192.165 & 40.6573 & -196.417 \\ -193.488 & -41.0585 & 197.799 \end{pmatrix}$$

practically simple algorithm is explained. Also a novel and powerful geometric tool called variational Ricci flow is introduced, which is efficient, robust and easy to implement.

In the future, we will focus on designing novel spline schemes which are based on hyperbolic structures or real projective structures, and constructing manifold splines without extraordinary points. We also prove whether the discrete Ricci Flow will converge, as one refines the meshes approximating a smooth surface, toward the smooth Ricci Flow.

Acknowledgement

We thank Stanford university and Cindy Grimm for the surface models.

This work was partially supported by the NSF CAREER Award CCF-0448339 and NSF DMS-0528363 to X. Gu.

References

- BENZÈCRI, J. P. 1959. Varits localement affines. *Sem. Topologie et Gom. Diff., Ch. Ehresmann* 7, 229–332.
- BOBENKO, A., AND SCHRODER, P. 2005. Discrete willmore flow. In *Eurographics Symposium on Geometry Processing*.
- BOBENKO, A. I., AND SPRINGBORN, B. A. 2004. Variational principles for circle patterns and koebe's theorem. *Transactions of the American Mathematical Society* 356, 659.
- CARNER, C., JIN, M., GU, X., AND QIN, H. 2005. Topology-driven surface mappings with robust feature alignment. In *IEEE Visualization*, 543–550.
- CHOW, B., AND LUO, F. 2003. Combinatorial ricci flows on surfaces. *Journal Differential Geometry* 63, 1, 97–129.
- COLIN DE VERDIÈRE, É., AND LAZARUS, F. 2002. Optimal system of loops on an orientable surface. In *Proceedings of the 43rd Annual IEEE Symposium on Foundations of Computer Science*, 627–636.
- DAI, J., LUO, W., YAU, S.-T., AND GU, X. 2006. Geometric accuracy analysis for discrete surface approximation. In *Geometric Modeling and Processing*. submitted.
- DE VERDIÈRE, C. 1991. Yves un principe variationnel pour les empilements de cercles. (french) "a variational principle for circle packings". *Invent. Math.* 104 3, 655–669.
- ERICKSON, J. G., AND WHITTLESEY, K. 2005. Greedy optimal homotopy and homology generators. In *Proc. 16th Symp. Discrete Algorithms*, ACM and SIAM, 1038–1046.
- FERGUSON, H., ROCKWOOD, A. P., AND COX, J. 1992. Topological design of sculptured surfaces. In *SIGGRAPH*, 149–156.
- GOLDMAN, R. 2003. Computer graphics in its fifth decade: Ferment at the foundations. In *11th Pacific Conference on Computer Graphics and Applications (PG'03)*, 4–21.
- GOTSMAN, C., GU, X., AND SHEFFER, A. 2003. Fundamentals of spherical parameterization for 3d meshes. *ACM Trans. Graph.* 22, 3, 358–363.
- GRIMM, C., AND HUGHES, J. F. 2003. Parameterizing n-holed tori. In *IMA Conference on the Mathematics of Surfaces*, 14–29.
- GU, X., AND YAU, S.-T. 2003. Global conformal parameterization. In *Symposium on Geometry Processing*, 127–137.
- GU, X., WANG, Y., CHAN, T. F., THOMPSON, P. M., AND YAU, S.-T. 2004. Genus zero surface conformal mapping and its application to brain surface mapping. *IEEE Trans. Med. Imaging* 23, 8, 949–958.
- GU, X., HE, Y., AND QIN, H. 2005. Manifold splines. In *Symposium on Solid and Physical Modeling*, 27–38.
- HAKER, S., ANGENENT, S., TANNENBAUM, A., KIKINIS, R., SAPIRO, G., AND HALLE, M. 2000. Conformal surface parameterization for texture mapping. *IEEE Trans. Vis. Comput. Graph.* 6, 2, 181–189.
- HAMILTON, R. S. 1988. The ricci flow on surfaces. *Mathematics and general relativity* 71, 237–262.

- JIN, M., WANG, Y., YAU, S.-T., AND GU, X. 2004. Optimal global conformal surface parameterization. In *IEEE Visualization*, 267–274.
- J.W.MILNOR. 1958. On the existence of a connection with curvature zero. *Comm. Math. Helv.* 32, 215–223.
- KHAREVYCH, L., SPRINGBORN, B., AND SCHRODER, P. 2005. Discrete conformal mappings via circle patterns.
- LUO, W., AND GU, X. 2006. Discrete curvature flow and derivative cosine law. In *preprint*.
- LUO, W. 2006. Error estimates for discrete harmonic 1-forms over riemann surfaces. In *Communications in Analysis and Geometry*. submitted.
- MUNKRES, J. 1984. *Elements of Algebraic Topology*. Addison-Wesley Co.
- PETERSEN, P. 1997. *Riemannian Geometry*. Springer Verlag.
- PRAUN, E., AND HOPPE, H. 2003. Spherical parametrization and remeshing. *ACM Trans. Graph.* 22, 3, 340–349.
- RATCLIFFE, J. G. 1994. *Foundations of Hyperbolic Manifolds*. Springer Verlag.
- RODIN, B., AND SULLIVAN, D. 1987. The convergence of circle packings to the riemann mapping. *Journal of Differential Geometry* 26, 2, 349–360.
- SOVAKAR, A., AND KOBELT, L. 2004. Api design for adaptive subdivision schemes. *Computers & Graphics* 28, 1, 67–72.
- STEPHENSON, K. 2005. *Introduction To Circle Packing*. Cambridge University Press.
- THURSTON, W. 1976. *Geometry and Topology of 3-manifolds*. Princeton lecture notes.
- THURSTON, W. P. 1997. *Three-Dimensional Geometry and Topology*. Princeton University Press.
- WALLNER, J., AND POTTMANN, H. 1997. Spline orbifolds. *Curves and Surfaces with Applications in CAGD*, 445–464.

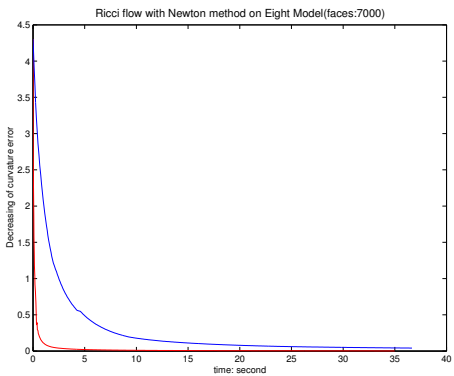


Figure 9: Comparison of performance of Ricci flow with Newton's method (lower red curve) over the gradient descent method (upper blue curve). Both converge exponentially.



Figure 10: The spherical structure and real projective structure of a genus zero closed surface.

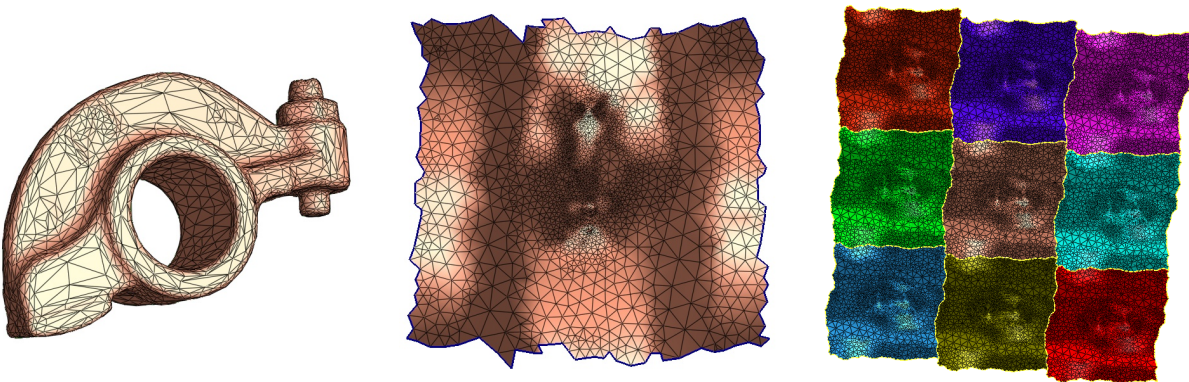


Figure 3: **The Euclidean structure of a genus one closed surface:** (a) the original surface (b) one fundamental domain (c) part of its universal covering space

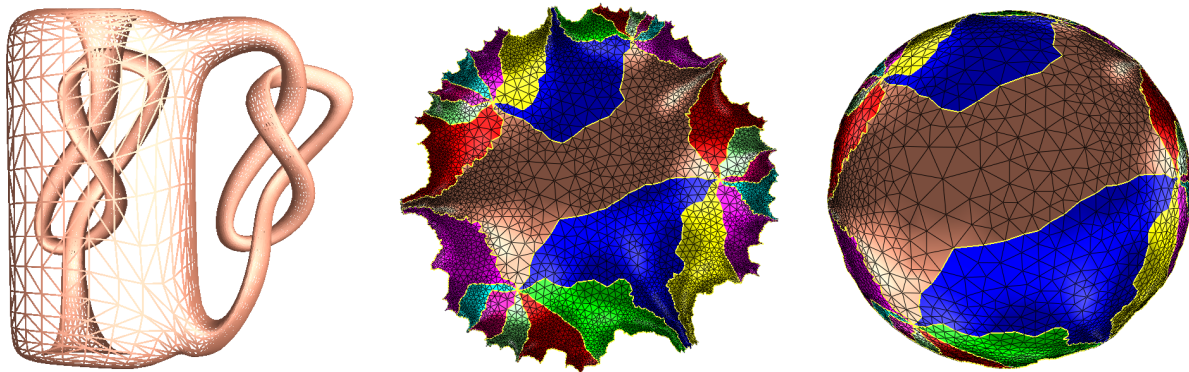


Figure 4: **The hyperbolic structure of a genus two closed surface:** (a) the original surface (b) the isometric embedding of its universal covering space in the Poincaré disk (c) the isometric embedding in the Klein disk which induces real projective structures

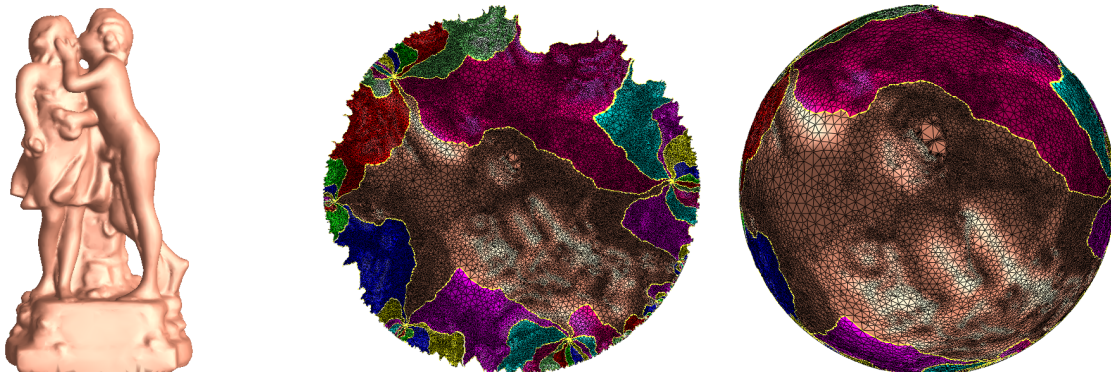


Figure 5: **The hyperbolic structure of a genus three closed surface:** (a) the original surface (b) the isometric embedding of its universal covering space in the Poincaré disk (c) the isometric embedding in the Klein disk which induces real projective structures

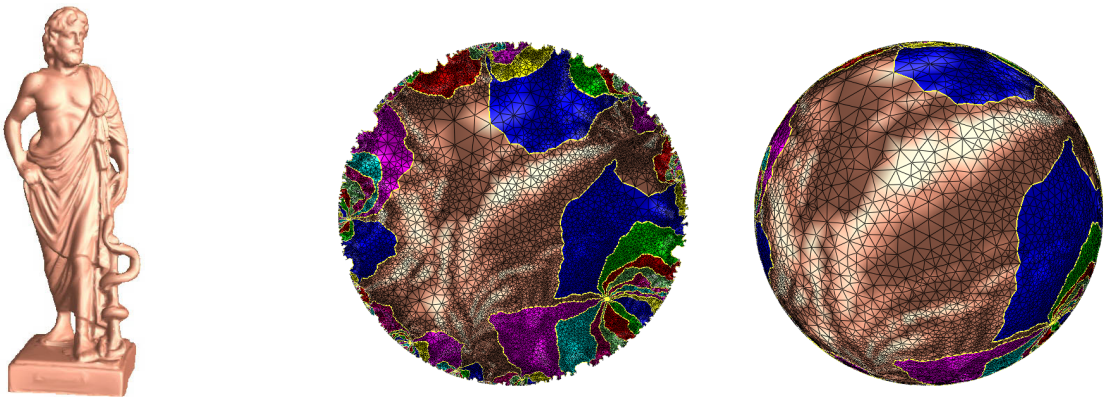


Figure 6: The hyperbolic structure of a genus four closed surface: (a) the original surface (b) the isometric embedding of its universal covering space in the Poincaré disk (c) the isometric embedding in the Klein disk which induces real projective structures

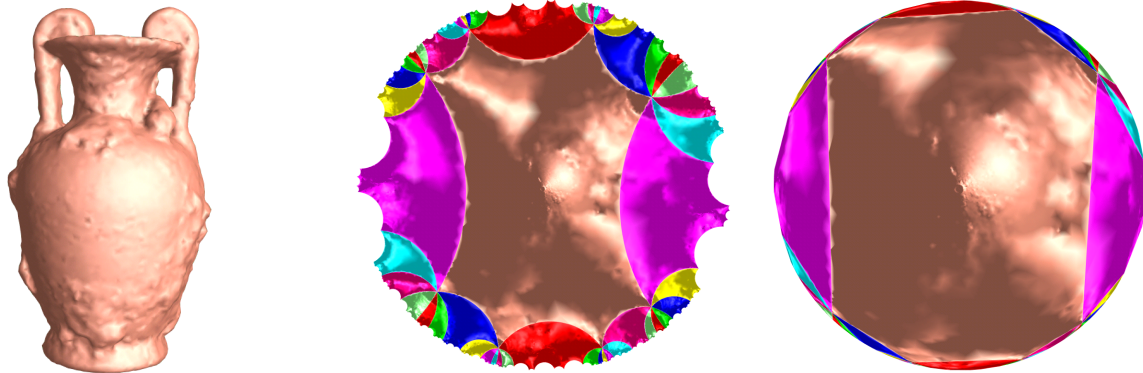


Figure 7: The hyperbolic structure of a genus two closed surface: (a) the original surface (b) the isometric embedding of its universal covering space in the Poincaré disk (c) the isometric embedding in the Klein disk which induces real projective structures. The boundaries of fundamental domains are straightened to hyperbolic lines.

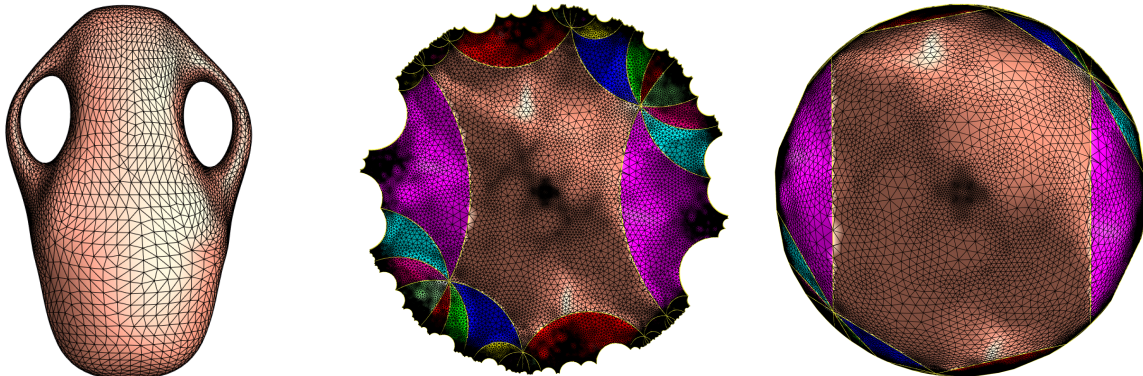


Figure 8: The hyperbolic structure of a genus two closed surface: (a) the original surface (b) the isometric embedding of its universal covering space in the Poincaré disk (c) the isometric embedding in the Klein disk which induces real projective structures. The boundaries of fundamental domains are straightened to hyperbolic lines.